

Reversible Isothermal Twist–Bend Nematic–Nematic Phase Transition Driven by the Photoisomerization of an Azobenzene-Based Nonsymmetric Liquid Crystal Dimer

Daniel A. Paterson,^{†,‡} Jie Xiang,[‡] Gautam Singh,[§] Rebecca Walker,[†] Deña M. Agra-Kooijman,[§] Alfonso Martínez-Felipe,[#] Min Gao,[‡] John M. D. Storey,[†] Satyendra Kumar,[§] Oleg D. Lavrentovich,[‡] and Corrie T. Imrie^{*,†}

[†]Department of Chemistry, School of Natural and Computing Sciences, University of Aberdeen, Meston Building, Old Aberdeen AB24 3UE, United Kingdom

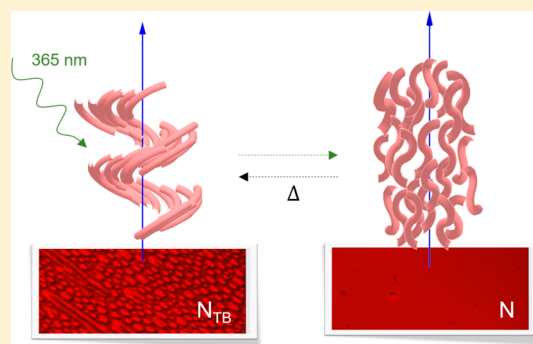
[‡]Liquid Crystal Institute and Chemical Physics Interdisciplinary Program, Kent State University, Kent, Ohio 44242, United States

[§]Department of Physics, Kent State University, Kent, Ohio 44242, United States

[#]School of Engineering, University of Aberdeen, King's College, Aberdeen AB24 3UE, United Kingdom

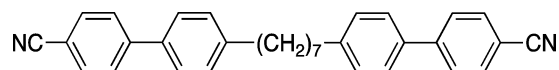
Supporting Information

ABSTRACT: The liquid crystal nonsymmetric dimer, 1-(4-butoxyazobenzene-4'-yloxy)-6-(4-cyanobiphenyl-4'-yl) hexane (CB6OABOBu), shows enantiotropic twist–bend nematic, N_{TB} , and nematic, N , phases. The N_{TB} phase has been confirmed using polarized light microscopy, freeze fracture transmission electron microscopy, and X-ray diffraction. The helicoidal pitch in the N_{TB} phase is 18 nm. The N_{TB} – N (T_{NTBN}) and N – I (T_{NI}) transition temperatures are reduced upon UV light irradiation, with the reduction in T_{NTBN} being much larger than that in T_{NI} . An isothermal, reversible N_{TB} – N transition may be driven photochemically. These observations are attributed to a trans–cis photoisomerization of the azobenzene fragment on UV irradiation, with the cis isomers stabilizing the standard nematic phase and the trans isomers stabilizing the N_{TB} phase. The dramatic changes in T_{NTBN} provide evidence that the transition between the normal nematic and twist–bend nematic with spontaneous breaking of chiral symmetry is crucially dependent on the shape of molecular dimers, which changes greatly during the trans–cis isomerization.



INTRODUCTION

Meyer¹ and Dozov² predicted the existence of spatially deformed nematic phases by suggesting that certain mesogenic molecules might have a tendency to pack into bent structures. Pure uniform bend in space is impossible; thus, the spontaneous bend must be accompanied by other deformations of the local director, either twist or splay, giving rise to the so-called twist–bend nematic, N_{TB} , or splay–bend nematic phases, respectively. In the N_{TB} phase, the director forms a conical left- or right-handed helix (Figure 1). The handedness is established spontaneously because the molecules are not chiral.



The helicoidal N_{TB} phase was identified for 1,7-bis-4-(4'-cyanobiphenyl) heptane, CB7CB.^{3–5} The CB7CB molecule is a dimer formed by two mesogenic cyanobiphenyl rigid units linked by a flexible spacer.^{6,7} The two mesogenic units are oblique with respect to each other when the odd-membered alkyl spacer is in

the all-trans conformation. This bent molecular shape is thought to be a prerequisite for the formation of the N_{TB} phase. Although molecules will have other non-trans conformations, the ensemble average of the molecular shape will be bent. This in turn can lead to packing with spontaneous bend, especially at high densities, thus triggering a transition from a standard nematic with a globally uniform director orientation to N_{TB} with local twists and bends. In the standard nematic, the tendency of molecules to bend is reflected in low values of the bend elastic constant.^{4,8,9}

The existence of a low-temperature nematic phase different from the conventional uniaxial phase had previously been reported in a number of earlier experimental works.^{10–12} However, it was only very recently that the nanoscale imaging by transmission electron microscopy allowed one to conclude that the low-temperature nematic exhibits periodic modulation of the director on the scale of nanometers^{4,5} and that these modulations are of the twist–bend type.⁴

Received: December 21, 2015

Published: March 25, 2016

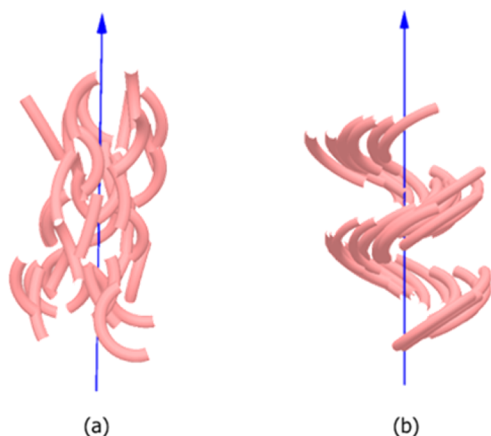
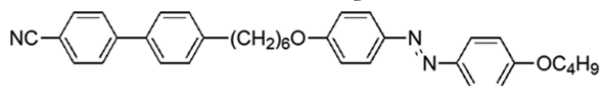


Figure 1. Schematic representations of (a) the nematic, N, and (b) the twist-bend nematic, N_{TB} , phases composed of bent molecules.

Currently, very few liquid crystal dimers have been reported to show the N_{TB} phase.^{3–5,8,13–18} Other examples of twist-bend nematogens include two liquid crystal trimers^{19,20} and a rigid bent-core liquid crystal.²¹ Given such a small data set of molecular structures, our understanding of the empirical relationships between molecular structure and the formation of this fascinating new phase is in a very early stage of development. What appears to be clear, however, is that a bent molecular shape is essential²² and that macroscopically this yields not only the thermodynamically stable N_{TB} phase but also a standard nematic with an anomalously small bend elastic constant.^{4,23,24} The latter feature leads to interesting electro-optical effects in a nematic doped with chiral dopants, such as electrically controlled selective reflection of light.²⁵

In designing new twist-bend nematogens, there exists the intriguing possibility of manipulating molecular shape using external stimuli in order to control the N_{TB} and N phases and their elastic properties. A possible way of achieving this is to utilize the photochemically driven trans-cis isomerization seen for azobenzene-based compounds.²⁶ The well-known effect of trans-to-cis isomerization in these compounds results in lowering of the nematic-isotropic transition temperature; the phenomenon is easy to explain by the extended shape of trans isomers and bent shape of cis isomers. However, other compounds exhibit an opposite behavior, with cis isomers stabilizing the nematic phase.²⁷ These prior results, however, do not provide any definite clues as to what effect trans-cis isomerization might have on a phase transition between the standard nematic phase and its twist-bend counterpart, a transition that is accompanied by the spontaneous chiral symmetry breaking and is thus potentially more sensitive to the fine details of molecular structures than the nematic-to-isotropic transition.



To explore the effects of photoisomerization on the $N-N_{TB}$ phase transition, we have synthesized and characterized a dimer containing an azobenzene moiety, namely, 1-(4-butoxyazobenzene-4'-yloxy)-6-(4-cyanobiphenyl-4'-yl) hexane, referred to by the acronym CB6OABOBu. Our study demonstrates a profound effect of photoisomerization, with cis isomers favoring the N phase and trans isomers favoring the N_{TB} phase.

RESULTS AND DISCUSSION

The phases, transition temperatures, and transition enthalpies of CB6OABOBu are listed in Table 1, and Figure 2 shows the

Table 1. Phase Behavior of CB6OABOBu^a

T_{Cr} (°C)	T_{NTBN} (°C)	T_{NI} (°C)	ΔH_{Cr} (kJ mol ⁻¹)	ΔH_{NTBN} (kJ mol ⁻¹)	ΔH_{NI} (kJ mol ⁻¹)
104.8	105.5	152.7	49.40	0.06	1.43

^aData extracted from DSC measurements on heating at 10 °C/min.

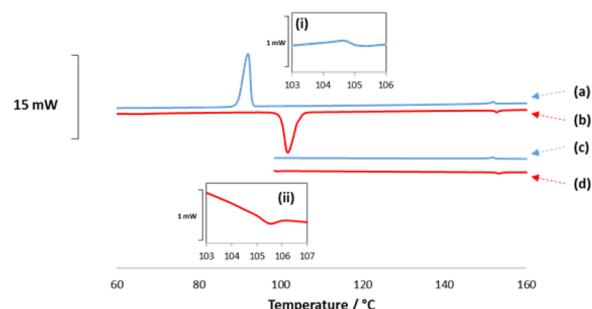


Figure 2. DSC scans of CB6OABOBu obtained during (a) first cooling, (b) subsequent reheating, (c) second cooling to 100 °C without crystallization, (d) reheating immediately after c. The insets magnify the weak $N_{TB}-N$ peak seen (i) during the cooling trace shown in c and (ii) on reheating shown in d. All heating and cooling rates: 10 °C min⁻¹.

associated DSC traces. The enthalpy change associated with the $N-N_{TB}$ transition is very small (Figure 2). The N phase was identified on the basis of the polarizing microscopic observation of characteristic director fluctuations and Schlieren texture containing both two- and four-brush singularities (Figure 3a). On cooling, the Schlieren texture changed to give rise to regions of fanlike textures with nonperiodic stepped edges in coexistence with a striated texture (Figure 3b) characteristic of the N_{TB} phase.¹⁵ In all cases, the formation of the N_{TB} phase is accompanied by the cessation of optical flickering associated with director fluctuations of the conventional nematic phase.

To study the optical textures of CB6OABOBu in the absence of the effects of UV light, a red color filter was used. Figure 4 shows the optical textures for a planar-aligned sample in a rubbed PI2555 cell ($d = 12 \mu\text{m}$) with a red color filter (>600 nm light allowed through). Uniform alignment of the sample in the N phase is seen in Figure 4c. On entering the N_{TB} phase, a striped texture develops parallel to the rubbing direction, characteristic of the N_{TB} phase (Figure 4d). The formation of the N_{TB} phase is visible as a propagating front that separates the conventional N phase with optical flickering of the textures, associated with director fluctuations, and flickering- and fluctuation-free N_{TB} texture with “frozen” defects such as focal conic domains and stripes described for other N_{TB} materials.^{3,4} We will return to a discussion of the effect of light on the phase behavior of CB6OABOBu later.

The layered structure of the N_{TB} phase is clearly evidenced in freeze fracture transmission electron microscopy (FFTEM) images of Pt/C replicas of the fractured sample, Figure 5. The periodic pattern (Figure 5a) observed in the TEM textures corresponds to the variable director tilt with respect to the plane of view. The textures in Figure 5a correspond to the field of view that is parallel to the heliconical axis of the N_{TB} phase.⁴ Variable tilt of the director results in local ridges and valleys of the fracture; their presence is visualized by the Pt/C deposits that

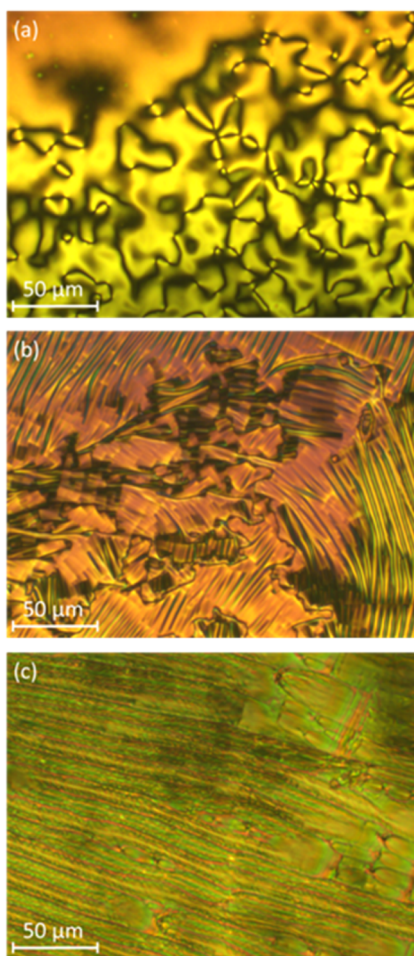


Figure 3. Optical textures of (a) the nematic phase (151 °C), (b) the twist-bend nematic phase (89 °C), and (c) the twist-bend nematic phase (103 °C) observed without the red color filter for CB6OABOBu.

form a thicker film on one side of the ridges; the periodicity of the dark and bright regions of the replica corresponds to the pitch of the heliconical structure. The pitch determined from the TEM textures of the replicas is around 18 nm, i.e., about twice the TEM textures of the replicas is shown by CB7CB.^{4,5} It is important to note that if the CB6OABOBu samples are prepared under ambient light conditions (without filters), the corresponding fractures show no periodic features (Figure 5b); the latter strongly suggests that ambient light causes a transformation of the N_{TB} phase into the conventional uniaxial N phase.

Two representative X-ray diffraction patterns obtained for the N and N_{TB} phases are shown in Figure 6, and in both, two pairs of diffuse peaks in orthogonal directions are observed confirming the presence of the orientational order. It should be noted that in general an aligned high-temperature LC phase loses the alignment across a first-order phase transition as the director distribution is uncontrollable and weak external fields may not influence the lower phase alignment. To ensure that all measurements reported here were made on sample volumes that remained aligned across the transition, we employed a very narrow X-ray beam and monitored the sample mosaicity across the transition. All data presented here are from measurement cycles during which the sample alignment remained unchanged.

The length scales (or d spacings) corresponding to the small- and large-angle peaks are 15.9 ± 0.1 and 4.55 ± 0.05 Å, respectively. Below 110 °C, the large-angle reflections become

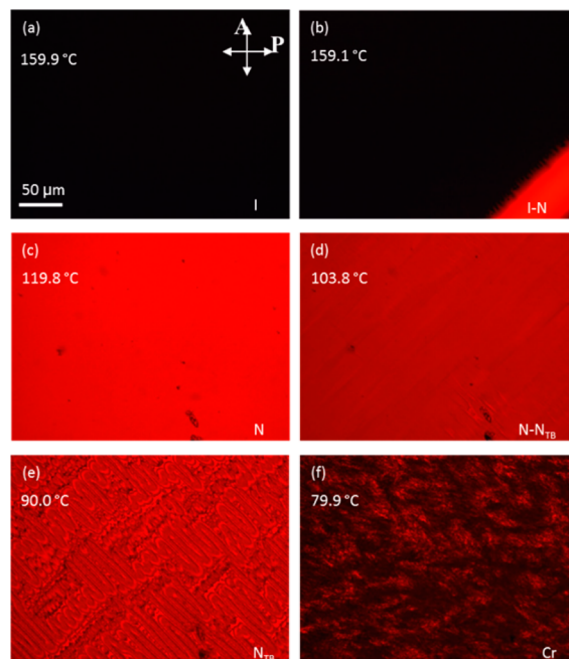


Figure 4. Optical textures of (a) the isotropic phase (159.9 °C), (b) the isotropic–nematic phase transition (159.1 °C), (c) the nematic phase (119.8 °C), (d) twist–bend nematic phase (103.8 °C), (e) deep within the twist–bend nematic phase (90.0 °C), and (f) the crystal phase (79.9 °C) observed for CB6OABOBu in a 12 μm PI2555 cell with a red color filter (>600 nm light allowed through).

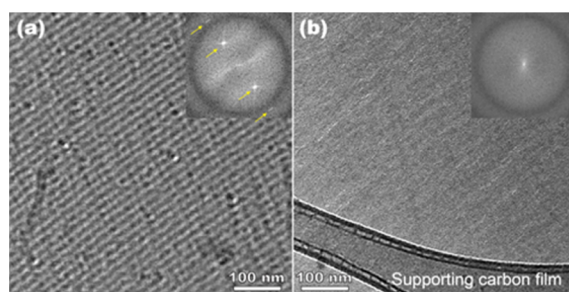


Figure 5. Representative FFTEM images of the samples fractured (a) without and (b) with ambient light. The insets correspond to fast Fourier transform patterns. The sharp bright spots (marked by arrows) indicate a well-defined 1D modulation with a periodicity of approximately 18 nm.

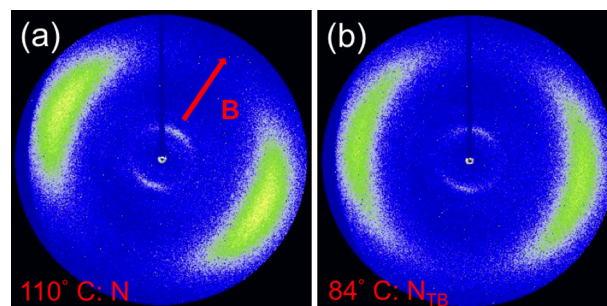


Figure 6. Diffraction patterns in the (a) N and (b) N_{TB} phase of a magnetic field (shown by the red arrow marked B) aligned sample of CB6OABOBu.

wider (Figure 6b), but the small-angle reflections remain more or less unaffected. There were no condensed smectic-like peaks

observed up to 100 Å. The estimated molecular length of CB6OABOBu with the spacer in the all-trans conformation is about 32 Å, indicating that at a local level the structure in the N and N_{TB} phases is intercalated; this appears to be a general observation in dimers exhibiting N_{TB} behavior. Because the most profound effect of UV exposure occurs in the N_{TB} phase, the sample was exposed to different brilliance of UV radiation as discussed in section 1.5 of the Supporting Information. The red symbols shown in Figure 7 correspond to order parameters at two different N_{TB} temperatures when irradiated with 2.5 mW/cm² of UV.

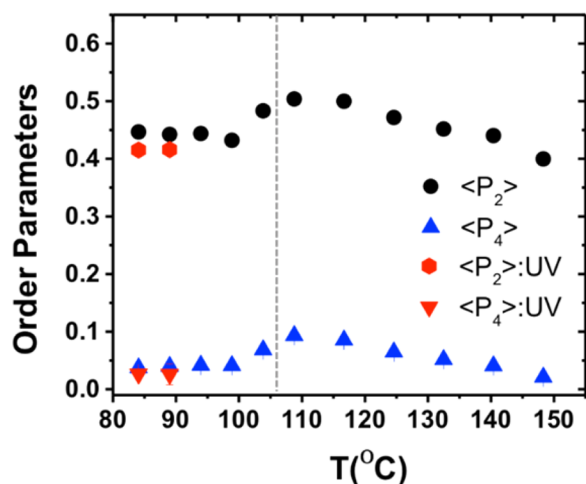


Figure 7. Temperature dependence of orientational order parameters $\langle P_2(\cos \theta) \rangle$ and $\langle P_4(\cos \theta) \rangle$ in nematic phases of CB6OABOBu sample.

Azimuthal scans (often referred to as χ scans) generated from the large-angle peaks were analyzed using the numerical inversion method of Davidson et al.,²⁸ which has been applied to calamitic, phasmidic, and polymeric mesogens, to calculate the nematic order parameters $\langle P_2(\cos \theta) \rangle$ and $\langle P_4(\cos \theta) \rangle$ as functions of temperature, shown in Figure 7. The order parameter $\langle P_6(\cos \theta) \rangle$ remained essentially zero in both phases. Both order parameters increase monotonically with decreasing temperature in the N phase as one would expect. However, the values of both $\langle P_2(\cos \theta) \rangle$ and $\langle P_4(\cos \theta) \rangle$ show a marked decrease between 105 and 110 °C, i.e., at the transition to the N_{TB} phase. The decrease continues in the N_{TB} phase. The temperature dependence of these two parameters is similar to that reported for the CB7CB+CB6CB mixtures, and $\langle P_2(\cos \theta) \rangle$ is semiquantitatively in agreement with previous NMR measurements²⁹ on CB7CB. The behavior is also consistent with the experimentally measured decrease in birefringence of the nematic phase near the N–N_{TB} phase transition.^{4,30} These order parameters are found to decrease slightly upon exposure to UV light (red symbols in Figure 7), suggesting a slight disordering of the phase. However, it appears that the changes that occur upon UV irradiation are more on a macroscopic scale as no significant changes in the molecular organization and order parameters are discernible at this phase transition.

We now return to consider the effects of UV light on the phase behavior of CB6OABOBu. The reversible nature of this isothermal, photochemically driven N_{TB}–N phase transition is evident in Figure 8. Thus, Figure 8a shows the optical texture when viewed through the polarized light microscope with a red color filter on cooling the sample into the N_{TB} phase. The sample

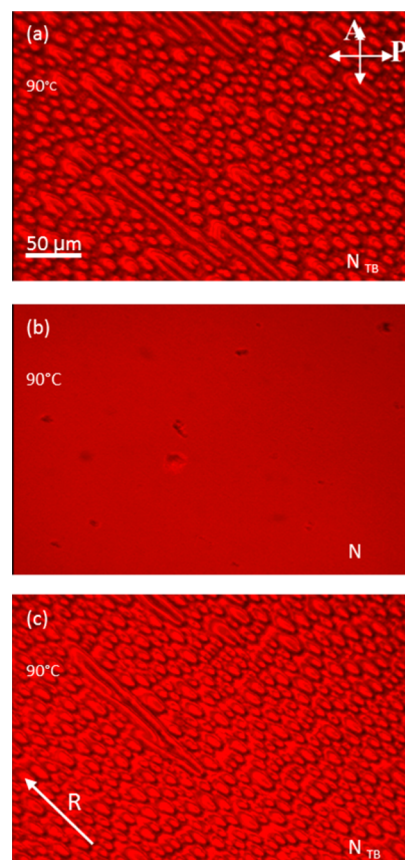


Figure 8. Optical textures of CB6OABOBu confined in a 12 μm cell obtained for (a) the N_{TB} phase on cooling from the isotropic phase, (b) the N phase after about 30 s exposure to UV of intensity 1 mW cm^{−2}, and (c) the N_{TB} phase formed in 15 s after removing the UV source. The textures are of the same area of the sample at 90 °C. R indicates the rubbing direction.

was irradiated using a UV light source of intensity 1 mW cm^{−2}. After about 30 s of light exposure, the sample had undergone a transition into the nematic phase (Figure 8b). The light was switched off, and in about 15 s, the N_{TB} phase reappeared (Figure 8c).

The N_{TB} textures in Figures 8a,c exhibit focal conic domains similar to those observed in smectics and short-pitch cholesterics. Although the two textures are different in details, they have a common feature: the long axes of the elliptic bases of the focal conic domains are parallel to the direction of rubbing. This alignment is dictated by geometry of the domains; the normals to the N_{TB} pseudolayers lie in the plane of the elliptical base and run along the radial lines emanating from one of the two foci of the ellipse.³¹ As a result, the in-plane surface anchoring energy is minimized when the long axis of the ellipse is parallel to the rubbing direction, as observed in Figures 8a,c. Focal conic domain textures in other N_{TB} materials show similar alignment.³² Because the UV irradiation does not change the direction of rubbing, the focal conic textures before and after irradiation show similarly arranged focal conic domains.

The change in the phase behavior of azobenzene-based liquid crystals induced by UV light is attributed to the photoisomerization of the azo-linkage and the concurrent change in molecular shape (Figure 9). To verify that CB6OABOBu undergoes photochemical isomerization, we measured the UV–vis spectra of the material at 90 °C, i.e., in the N_{TB} phase,

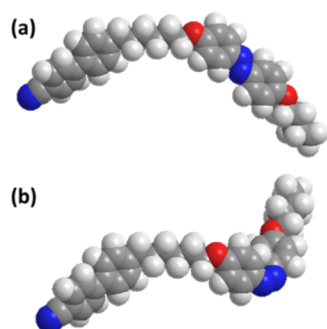


Figure 9. Space-filling molecular models for CB6OABOBu with the azobenzene moiety in the (a) trans and (b) cis conformations.

before and after exposure to UV light of wavelength 365 nm (Figure 10). Prior to irradiation, the UV-vis spectrum contains a

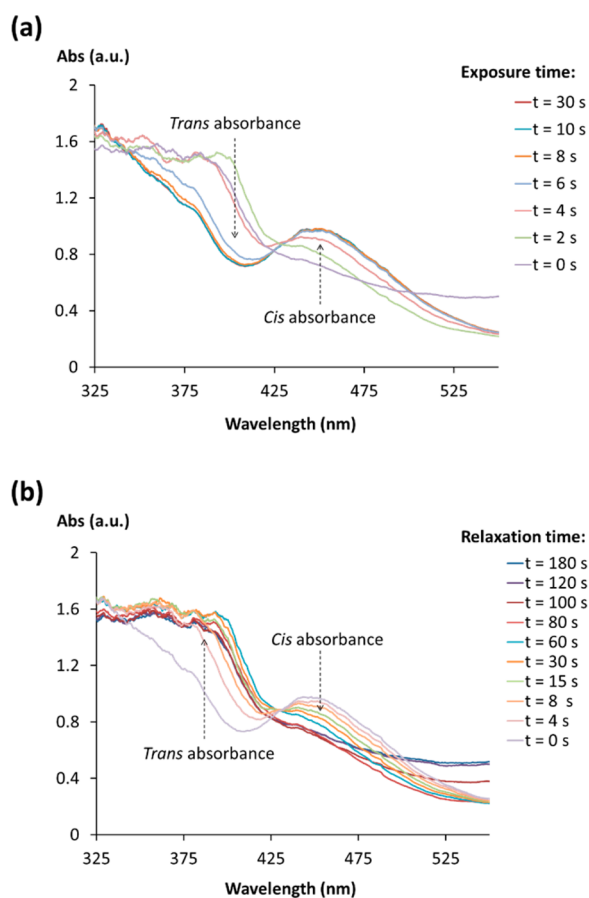


Figure 10. UV-vis spectrum of CB6OABOBu in a 1.7 μm quartz cell at 90 $^{\circ}\text{C}$ (a) during irradiation by UV light of wavelength 365 nm and intensity 30 mW cm^{-2} and (b) after turning the UV light off.

strong peak at around 365 nm associated with the π - π^* transition of the trans form and a much smaller peak at around 450 nm associated with the weak, symmetry forbidden π - π^* transition of the cis form. Irradiation causes the amplitude of the 365 nm peak to decrease and that of the 450 nm peak to increase, indicating trans-cis photoisomerization of the azobenzene units (Figure 10a). The peaks evolve with the exposure time and saturate after about 30 s. When the UV irradiation is switched off, a slow thermal cis-trans relaxation is observed, manifested by an

increase in the intensity of the 365 nm band and a simultaneous decrease of the 450 nm peak (Figure 10b).

Figure 11a shows the time taken for a given intensity of UV light to drive the N_{TB} -N and N-I phase transitions at 90 $^{\circ}\text{C}$; for

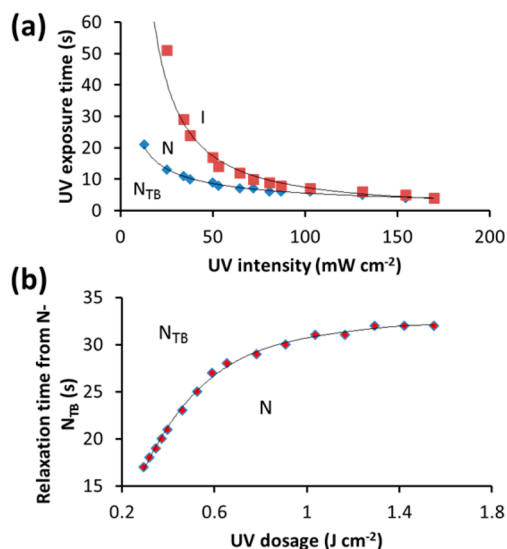


Figure 11. Dependence of (a) the time taken to drive the N_{TB} -N and N-I phase transitions on the intensity of the UV light and (b) the time required for the back relaxation to form the N_{TB} phase as a function of applied UV dosage using a UV source of intensity 12.8 mW cm^{-2} . All measurements were recorded at 90 $^{\circ}\text{C}$ with the sample in a 12 μm planar aligned cell.

example, for a UV light intensity of 50.1 mW cm^{-2} , it takes around 9 s to convert the N_{TB} phase into the N phase and a further 8 s to obtain the I phase. A considerably lower UV dosage is required to drive the N_{TB} -N than the N-I transition. Figure 11b shows the dependence of the time taken after applying a given dosage of UV radiation to drive the formation of the N phase to the reappearance of the N_{TB} phase. The time taken for the reappearance of the N_{TB} phase increases with the UV dosage applied and appears to reach a limiting value, presumably the photostationary concentration. We note that throughout these cycling experiments no appreciable changes in the transition temperatures were observed after leaving the samples overnight to relax, strongly suggesting that no chemical degradation had occurred during these experiments.

It is clear that the isothermal phase transitions observed for CB6OABOBu when illuminated by UV light are driven by changes in the concentration of the cis isomer (Figure 10). In particular, cis isomers destabilize the N_{TB} phase toward a formation of the standard N phase and then destabilize the N phase by causing a transition to the isotropic phase. Although the second transition is not surprising and has been observed for other azobenzene-based nematics, destabilization of N_{TB} is rather surprising. To explain it qualitatively, we must consider the shapes of the trans and cis isomers, Figure 9. In the trans form, the molecular bend is governed by the geometry of the spacer giving a spatially uniform bend. By comparison, in the cis isomer the bent fragments occur at two different locations (the azobenzene moiety and the spacer), causing a reverse in the bend polarity as one moves from one end of the molecule to the other end. Such a spatially varying bend is hardly compatible with local packing requirements of the N_{TB} phase.

CONCLUSIONS

We have shown that CB6OABOBu exhibits the fascinating twist–bend nematic phase, N_{TB} , and that this may be attributed largely to the bent shape of the trans isomer of the molecule. The material shows an isothermal N_{TB} – N transition when illuminated by UV light that is driven by the photoisomerization of the azo linkage generating the cis isomer. This transition is reversible on removing the light source driven by the thermal relaxation giving the trans isomer. At higher concentrations of cis isomers, one observes a classic effect of the nematic–isotropic phase transition, described for other azobenzene-based liquid crystals. In principle, one might expect the cis isomers to enhance the tendency to form the N_{TB} phase because these are generally more strongly bent than the trans isomers. However, our findings indicate clearly that in the studied material with molecules that combine a flexible aliphatic bridge and the azobenzene moieties the cis isomer suppresses the N_{TB} phase in favor of the N phase. We attribute this to the particular shape of the cis isomer of CB6OABOBu, in which the polarity of bend is different in the aliphatic and azobenzene parts of the molecule. This prompts the fascinating question, however, as to whether the photocontrolled shape of CB6OABOBu can be used to control the bend elastic constant in the nematic phase and selective reflection of light in its chiral version; such studies are underway.

ASSOCIATED CONTENT

Supporting Information

The Supporting Information is available free of charge on the ACS Publications website at DOI: 10.1021/jacs.5b13331.

Materials used, synthetic procedures, methods for FFTEM, XRD, UV–vis spectroscopy and electro optic studies.(PDF)

AUTHOR INFORMATION

Corresponding Author

*c.t.imrie@abdn.ac.uk

Present Addresses

D.A.P., R.W., J.M.D.S., and C.T.I.: Department of Chemistry, School of Natural and Computing Sciences, University of Aberdeen, Meston Building, Old Aberdeen AB24 3UE, United Kingdom.

J.X., M.G., and O.D.L.: Liquid Crystal Institute and Chemical Physics Interdisciplinary Program, Kent State University, Kent, OH 44242, USA

G.S., D.M.A.-K., and S.K.: Department of Physics, Kent State University, Kent, OH 44242, USA.

A.M.-F.: School of Engineering, University of Aberdeen, King's College, Aberdeen, AB24 3UE, United Kingdom.

Notes

The authors declare no competing financial interest.

ACKNOWLEDGMENTS

D.A.P. would like to thank the RSC's mobility grant award scheme for funding of a research trip to the Liquid Crystal Institute at Kent State University. R.W. gratefully acknowledges the Carnegie Trust for the Universities of Scotland for the award of a vacation scholarship. G.S., D.M.A.-K., and S.K. gratefully acknowledge support for x-ray work from the Division of Basic Energy Sciences, Office of Science of the US Department of Energy under award DE-SC-0001412. ODL acknowledges support from NSF DMR-1410378 grant. The TEM data were

obtained at the TEM facility at the Liquid Crystal Institute, Kent State University, supported by the Ohio Research Scholars Program "Research Cluster on Surfaces in Advanced Materials".

REFERENCES

- (1) Meyer, R. B. In *Les Houches Summer School in Theoretical Physics*; Balian, R.G., Weil, G., Eds.; Gordon and Breach: New York, 1976; p 273.
- (2) Dozov, I. *Europhys. Lett.* **2001**, *56*, 247.
- (3) Cestari, M.; Diez-Berart, S.; Dunmur, D. A.; Ferrarini, A.; de la Fuente, M. R.; Jackson, D. J. B.; Lopez, D. O.; Luckhurst, G. R.; Perez-Jubindo, M. A.; Richardson, R. M.; Salud, J.; Timimi, B. A.; Zimmermann, H. *Phys. Rev. E* **2011**, *84*, 031704.
- (4) Borshch, V.; Kim, Y. K.; Xiang, J.; Gao, M.; Jakli, A.; Panov, V. P.; Vij, J. K.; Imrie, C. T.; Tamba, M. G.; Mehl, G. H.; Lavrentovich, O. D. *Nat. Commun.* **2013**, *4*, 2635.
- (5) Chen, D.; Porada, J. H.; Hooper, J. B.; Klittnick, A.; Shen, Y.; Tuchband, M. R.; Korblova, E.; Bedrov, D.; Walba, D. M.; Glaser, M. A.; MacLennan, J. E.; Clark, N. A. *Proc. Natl. Acad. Sci. U. S. A.* **2013**, *110*, 15931.
- (6) Imrie, C. T.; Henderson, P. A. *Chem. Soc. Rev.* **2007**, *36*, 2096.
- (7) Imrie, C. T.; Henderson, P. A.; Yeap, G.-Y. *Liq. Cryst.* **2009**, *36*, 755.
- (8) Adlem, K.; Copic, M.; Luckhurst, G. R.; Mertelj, A.; Parri, O.; Richardson, R. M.; Snow, B. D.; Timimi, B. A.; Tuffin, R. P.; Wilkes, D. *Phys. Rev. E* **2013**, *88*, 022503.
- (9) Cestari, M.; Frezza, E.; Ferrarini, A.; Luckhurst, G. R. *J. Mater. Chem.* **2011**, *21*, 12303.
- (10) Ungar, G.; Percec, V.; Zuber, M. *Macromolecules* **1992**, *25*, 75.
- (11) Sepelj, M.; Lesac, A.; Baumeister, U.; Diele, S.; Nguyen, H. L.; Bruce, D. W. *J. Mater. Chem.* **2007**, *17*, 1154.
- (12) Panov, V. P.; Nagaraj, M.; Vij, J. K.; Panarin, Y. P.; Kohlmeier, A.; Tamba, M. G.; Lewis, R. A.; Mehl, G. H. *Phys. Rev. Lett.* **2010**, *105*, 167801.
- (13) Tripathi, C. S. P.; Losada-Perez, P.; Glorieux, C.; Kohlmeier, A.; Tamba, M.-G.; Mehl, G. H.; Leys, J. *Phys. Rev. E* **2011**, *84*, 041707.
- (14) Mandle, R. J.; Davis, E. J.; Archbold, C. T.; Cowling, S. J.; Goodby, J. W. *J. Mater. Chem. C* **2014**, *2*, 556.
- (15) Mandle, R. J.; Davis, E. J.; Lobato, S. A.; Vol, C. C. A.; Cowling, S. J.; Goodby, J. W. *Phys. Chem. Chem. Phys.* **2014**, *16*, 6907.
- (16) Henderson, P. A.; Imrie, C. T. *Liq. Cryst.* **2011**, *38*, 1407.
- (17) Mandle, R. J.; Davis, E. J.; Archbold, C. T.; Voll, C. C. A.; Andrews, J. L.; Cowling, S. J.; Goodby, J. W. *Chem. - Eur. J.* **2015**, *21*, 8158.
- (18) Gorecka, E.; Vaupotic, N.; Zep, A.; Pocięcha, D.; Yoshioka, J.; Yamamoto, J.; Takezoe, H. *Angew. Chem., Int. Ed.* **2015**, *54*, 10155 We note that this reports a twist–bend nematogen containing an azobenzene-based mesogenic moiety but does not include a study of the effects of photoisomerization on phase behaviour.
- (19) Jansze, S. M.; Martinez-Felipe, A.; Storey, J. M. D.; Marcellis, A. T. M.; Imrie, C. T. *Angew. Chem., Int. Ed.* **2014**, *54*, 643.
- (20) Wang, Y.; Singh, G.; Agra-Kooijman, D. M.; Gao, M.; Bisoyi, H. K.; Xue, C.; Fisch, M. R.; Kumar, S.; Li, Q. *CrystEngComm* **2015**, *17*, 2778.
- (21) Chen, D.; Nakata, M.; Shao, R.; Tuchband, M. R.; Shuai, M.; Baumeister, U.; Weissflog, W.; Walba, D. M.; Glaser, M. A.; MacLennan, J. E.; Clark, N. A. *Phys. Rev. E* **2014**, *89*, 022506.
- (22) Lu, Z.; Henderson, P. A.; Paterson, B. J. A.; Imrie, C. T. *Liq. Cryst.* **2014**, *41*, 471.
- (23) Sebastian, N.; Lopez, D. O.; Robles-Hernandez, B.; de la Fuente, M. R.; Salud, J.; Perez-Jubindo, M. A.; Dunmur, D. A.; Luckhurst, G. R.; Jackson, D. J. B. *Phys. Chem. Chem. Phys.* **2014**, *16*, 21391.
- (24) Greco, C.; Luckhurst, G. R.; Ferrarini, A. *Soft Matter* **2014**, *10*, 9318.
- (25) Xiang, J.; Li, Y.; Li, Q.; Paterson, D. A.; Storey, J. M. D.; Imrie, C. T.; Lavrentovich, O. D. *Adv. Mater.* **2015**, *27*, 3014.
- (26) Bandara, H. M. D.; Burdette, S. C. *Chem. Soc. Rev.* **2012**, *41*, 1809.
- (27) Kosa, T.; Sukhomlinova, L.; Su, L.; Taheri, B.; White, T. J.; Bunning, T. J. *Nature* **2012**, *485*, 347.

- (28) Davidson, P.; Petermann, D.; Levelut, A. M. *J. Phys. II* **1995**, *5*, 113.
- (29) Mehl, G. H.; Tamba, M. G.; Joy, H.; Lelli, M.; Emsley, J. W. Lecture at *25th ILCC*, Dublin, Ireland, 2014.
- (30) Meyer, C.; Luckhurst, G. R.; Dozov, I. *J. Mater. Chem. C* **2015**, *3*, 318.
- (31) Kleman, M.; Lavrentovich, O. D. *Soft Matter Physics: An Introduction*; Springer: New York, 2003.
- (32) Challa, P. K.; Borshch, V.; Parri, O.; Imrie, C. T.; Sprunt, S. N.; Gleeson, J. T.; Lavrentovich, O. D.; Jakli, A. *Phys. Rev. E* **2014**, *89*, 060501.